# Magnetic Fe stripes created by self-organized MnAs template: Stripe edge pinning and high-frequency properties

S. Tacchi,[1,*] M. Madami,[1] G. Carlotti,[1] G. Gubbiotti,[1] M. Marangolo,[2] J. Milano,[3] R. Breitwieser,[2] V. H. Etgens,[2] R. L. Stamps,[4] and M. G. Pini[5]

[1]*CNISM, Dipartimento di Fisica, Università di Perugia, Via A. Pascoli, I-06123 Perugia, Italy*

[2]*INSP, UPMC Paris 06, CNRS UMR 7588, 140 Rue de Lourmel, 75015 Paris, France*

[3]*CNEA-CONICET and Instituto Balseiro, UNCuyo Centro Atómico Bariloche, R8402AGP San Carlos de Bariloche, Argentina*

[4]*School of Physics, University of Western Australia, 35 Stirling Highway, Crawley, Western Australia 6009, Australia*

[5]*Istituto dei Sistemi Complessi, CNR, Via Madonna del Piano 10, I-50019 Sesto Fiorentino, Italy*

(Received 22 July 2009; revised manuscript received 16 September 2009; published 13 October 2009)

Self-organization is an interesting route to the fabrication of nanostructured magnetic materials. Here we show that, near room temperature, an ultrathin Fe film deposited on a suitable MnAs template spontaneously breaks into a "lateral" superlattice of magnetic stripes. The magnetic superstructure originates from the temperature-dependent morphological change in the substrate: an epitaxially grown MnAs/GaAs(001) film, whose groove-ridge structure was investigated by scanning tunneling microscopy. Owing to the stray magnetic fields produced by the underlying MnAs template, the Fe stripe domains have opposite magnetizations, and behave essentially as independent magnetic entities because of strong stripe edge pinning. This is shown dramatically in terms of a split microwave resonance that can be controlled with an external magnetic field, as proved by Brillouin light-scattering data and analysis of the Fe spin-wave frequencies. Additionally, the potential for device applications of such lateral magnetic superlattices, displaying an "inverse" exchange-spring behavior, is discussed.

DOI: 10.1103/PhysRevB.80.155427 PACS number(s): 75.70.−i, 78.35.+c, 75.75.+a, 75.30.Ds

## I. INTRODUCTION

The lateral modulation of magnetic properties of thin films opens new opportunities for tuning their functionalities. A paradigmatic case is represented by exchange-spring magnets[1] and the emerging field of magnonics, where artificial magnonic crystals are used to control the generation and propagation of information-carrying spin waves.[2]

Nearly two decades ago, the concept of exchange-spring magnet was introduced[1] as a new tool to obtain cost-effective permanent magnets with high performance. The idea was to suitably disperse two ferromagnetic phases, each with different magnetic properties: for example, realizing an heterostructure[3] where a layer, made of a cheap 3*d*-transition-metal ferromagnetic material characterized by high-saturation magnetization and low magnetic anisotropy (soft phase), is alternated with another layer, made of a more expensive rare-earth-based ferromagnetic material with high anisotropy (hard phase). The exchange coupling between the two phases keeps their magnetizations aligned parallel in zero magnetic field and is responsible of a typical two-step demagnetization mechanism. In fact, when a nonzero field is applied antiparallel to the magnetization direction, the reversal of the magnetically soft phase takes place in a reversible way, while the magnetization of the hard phase keeps its former orientation. When the magnetic field is further increased over a critical value, an irreversible turn of the magnetization of the hard phase takes place. In this context Brillouin light scattering (BLS) was proved to be a quite useful tool to investigate the coupling of hard and soft ferromagnets in such "vertical" exchange-spring superlattices.[4]

Recent progress in nanostructuring techniques allowed the realization of a "lateral" exchange-spring superlattice: namely, using a patterned resist mask, a single-layer film made of parallel stripes of two magnetically different phases [$Ni_{81}Fe_{19}$ and $(Ni_{81}Fe_{19})_{94}Cr_6$, respectively] was obtained.[5] The stripes had fixed widths of 1000 nm and a height difference of 4 nm. In zero field the stripes had parallel aligned magnetizations and, for field applied along the stripe axis, magnetization reversal was shown to take place via a two-step process typical of magnetic exchange springs.

Here we discuss a very different possibility to realize, by means of self-organization, a lateral stripe-patterned superstructure in an ultrathin Fe film, taking advantage of the unusual and interesting temperature-dependent morphological change in an MnAs/GaAs(001) substrate.[6] The present BLS experiments and theoretical analysis show that the magnetizations of individual Fe stripes are effectively isolated from one another: in zero field the Fe stripes form an array of antiparallel magnetic domains (separated by 180° domain walls) that are stabilized via stray fields produced by the ferromagnetic MnAs substrate; for a sufficiently large applied magnetic field the stripes become parallel aligned. In some sense, the stripe-patterned Fe overlayer behaves like an "inverse" exchange spring: in fact, as mentioned above, in a conventional exchange spring the magnetizations of the two phases are parallel at zero field and become antiparallel at high magnetic field.

This first realization of a self-organized lateral exchange-springlike magnetic superlattice has potential applications for microwave devices, since the resonant response of this system is in the low GHz regime, an important area for microwave signal processing technologies. A challenge in this area for the creation of useful patterned materials for device applications, such as isolators and filters, is the large material volumes required. Fabrication costs for lithography can be

 

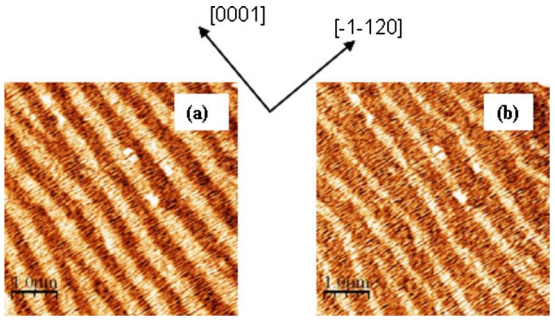


FIG. 1. (Color online) [(a) and (b)]: STM images of the 140-nm-thick MnAs/GaAs(001) template, obtained in constant current mode, at sample temperature $T_S$ of 308 and 313 K, respectively. Light-orange regions correspond to $\alpha$-MnAs and dark-orange ones to $\beta$-MnAs.

prohibitive and in this regard self-organization offers an attractive cost-effective means through which large-area lateral superlattices can be manufactured.

## II. EXPERIMENT

The sample was prepared at the Institut des NanoSciences de Paris. A 140-nm-thick MnAs layer was grown on GaAs(001) substrate by molecular-beam epitaxy, following the procedure in Ref. 9. A 4-nm-thick Fe film was then deposited onto MnAs kept at 150 °C and capped with 2 nm of Al for protection against oxidation. Transmission electron microscopy analysis shows that Fe epitaxially grows on MnAs with $(2,-1,1)_{\mathrm{Fe}}\|(1,1,0,0)_{\mathrm{MnAs}}\|(001)_{\mathrm{GaAs}}$ and $[11-1]_{\mathrm{Fe}}\|[0001]_{\mathrm{MnAs}}\|[110]_{\mathrm{GaAs}}$. Scanning tunneling microscopy (STM) measurements were performed in an ultrahigh-vacuum apparatus in constant current mode. The MnAs template exhibits a coexistence of an hexagonal ferromagnetic $\alpha$ phase with an orthorhombic nonferromagnetic $\beta$ one for a temperature range of about 40 K around RT, leading to the formation of a regular array of submicrometric stripes, where plateaus of $\alpha$ phase alternate periodically with shallow valleys of $\beta$ phase.[6,7] The width of the $\alpha$-MnAs stripes can be continuously tuned by changing temperature, whereas the stripe period, $P$, only depends on the film thickness, $t$, ($P \approx 5t$) and remains constant with temperature. Examples of the observed alternating-step configuration obtained by STM, are shown in Figs. 1(a) and 1(b) for the MnAs/GaAs(001) structure. The period of stripe pattern is $P=(650\pm 70)$ nm, while the height difference between $\alpha$ and $\beta$ phases is $h=(1.2\pm 0.2)$ nm, corresponding to less than 1% of MnAs film thickness ($t=140$ nm). The alternation of ferromagnetic $\alpha$-MnAs with paramagnetic $\beta$-MnAs has consequences for properties of the covering Fe film, which adopts the substrate morphology, changing from a continuous film into a parallel array of alternating steps, and is affected by the stray field produced by the underlying ferromagnetic $\alpha$-MnAs stripes.[8,9]

The dynamics of the Fe film has been studied by inelastic BLS, which provides frequencies for long wavelength, low-energy magnetic excitations. BLS measurements were carried out at the GHOST laboratory in Perugia.[10] A continuous flow optical cryostat was used to perform measurements as a function of temperature. About 200 mW of monochromatic $p$-polarized light, from a solid-state laser (532 nm line), was focused onto the sample surface using a camera objective. Note that with such an illuminating power, a local heating of about 40 K is induced in the probed region ($30\times 30$ $\mu$m$^2$). The backscattered light was analyzed by a Sandercock-type 3+3-pass tandem Fabry-Pérot interferometer. The external dc magnetic field was applied parallel to the surface of the film and perpendicular to the plane of incidence of light (i.e., in the so-called Damon-Eshbach geometry).

## III. RESULTS AND DISCUSSION

At a sample temperature $T_S=328$ K, where the MnAs substrate is fully in the $\beta$ phase (not shown here), the Fe layer is found to behave as a continuous film with in-plane anisotropy comprised of two parts: (i) a magnetocrystalline term,[11] associated with the $(2,-1,1)$ surface of bcc Fe film and (ii) a uniaxial contribution, whose easy axis $x=[0,1,1]_{\mathrm{Fe}}$, is perpendicular to the direction $y=[1,1,-1]_{\mathrm{Fe}}\|[0001]_{\mathrm{MnAs}}$, along which stripes develop upon reducing temperature. This uniaxial anisotropy is induced in the Fe film by the morphology of the MnAs substrate, which is characterized by the presence of a regular array of troughs perpendicular to the $[0001]_{\mathrm{MnAs}}$ direction.[9] Note that the Fe spin-wave frequencies, measured by BLS when the MnAs template is fully in either the $\alpha$ or $\beta$ phase (i.e., for $T_S<283$ K and $T_S>318$ K), are nearly identical[12] suggesting that the Fe anisotropies are independent of temperature over this range, in agreement with Ref. 7. Moreover, one can assume that direct interlayer exchange coupling between Fe and MnAs is negligible.

In the temperature range where the ferromagnetic and nonferromagnetic MnAs phases coexist, pairs of intensity peaks are found in the BLS spectra, as shown in the bottom insets of Figs. 2(a) and 2(b), revealing the existence of two distinct spin-wave modes. Their frequency evolution on decreasing the applied magnetic field strength $H$ is shown in Fig. 2 for sample temperature $T_S$ of 308 and 313 K, corresponding to different stripe widths. Having in mind the morphology of the underlying GaAs/MnAs substrate and the direction of its magnetization $M_\alpha$, sketched in Fig. 3, one can qualitatively attribute the presence of the two peaks to the two families of Fe stripes: (1) those lying between the $\alpha$-MnAs stripes, which experience a stray field $H_{stray,1}$ parallel to $M_\alpha$; (2) those located above the $\alpha$-MnAs stripes, which experience a stray field $H_{stray,2}$ antiparallel to $M_\alpha$.

From a quantitative point of view, analysis of the BLS results for the stripe configuration was done by first calculating the static magnetic configuration and effective fields acting in the Fe, and then fitting the experimental frequency data to the theoretical spin-wave frequencies. The system has been modeled as a regular array of infinitely long, alternating Fe/$\alpha$-MnAs and Fe/$\beta$-MnAs bilayered stripes (see Fig. 3). For such a structure, the Fe free-energy per unit volume can be written as

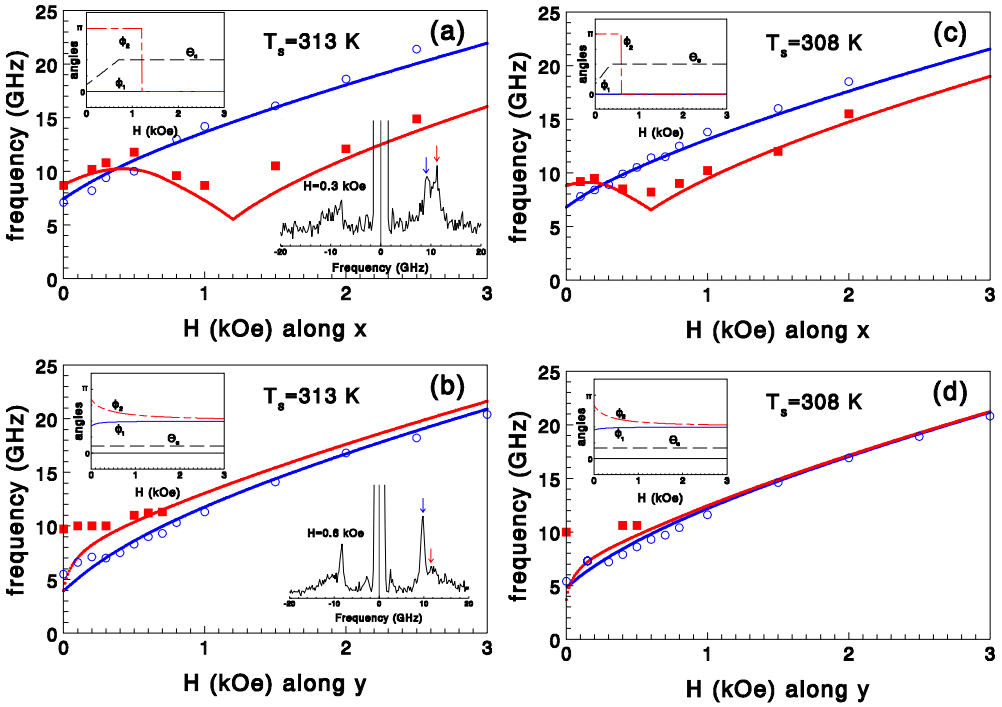


FIG. 2. (Color online) Field dependence of the measured Brillouin frequencies (symbols) of a 4-nm-thick Fe film deposited on the $\alpha$- and $\beta$-stripe phase of a 140-nm-thick film of MnAs/GaAs(001), (a) and (c) for $H$ along the $x$ and (b) and (d) for $H$ along the $y$ in-plane directions. Full lines: theoretical frequencies, $\omega_1$ (blue) and $\omega_2$ (red), calculated from Eq. (A2) with $q=1.67\times10^{-5}$ cm$^{-1}$ for $H$ along $x$ and $q=0$ for $H$ along $y$. Top insets: field dependence of the angles $\phi_1$, $\phi_2$, $\Theta_\alpha$ for field applied along $x$ and $y$, respectively. Bottom insets: BLS spectra displaying two peaks.

$$
\begin{aligned}
F = {} & \lambda_{12} M_1 M_2 [\sin\theta_1 \sin\theta_2 \cos(\phi_1 - \phi_2) + \cos\theta_1 \cos\theta_2] \\
& + \frac{1}{2} \sum_{i=1,2} M_i \left\{ \left( 4\pi M_S D_{z,i} - \frac{2K_{perp}}{M_S} \right) \cos^2\theta_i \right. \\
& + \left( 4\pi M_S D_{x,i} - \frac{2K_{paral}}{M_S} \right) \sin^2\theta_i \cos^2\phi_i \\
& - \frac{1}{12} \left( \frac{2K_1}{M_S} \right) [(3\cos^4\theta_i - 4\sqrt{2}\cos^3\theta_i \sin\theta_i \sin\phi_i \\
& + 6\cos^2\theta_i \sin^2\theta_i \cos^2\phi_i) \\
& + 12\sqrt{2}\sin^3\theta_i \cos\theta_i \sin\phi_i \cos^2\phi_i \\
& + \sin^4\theta_i (4\sin^4\phi_i + 3\cos^4\phi_i)] \\
& \left. - 2H \sin\theta_i \cos(\phi_i - \phi_H) - 2H^x_{stray,i} \sin\theta_i \cos\phi_i \right\}, \quad (1)
\end{aligned}
$$

where $M_1$ and $M_2$ are the magnetizations of Fe stripes deposited on $\beta$-MnAs and $\alpha$-MnAs stripes, respectively. $M_i$ $(i=1,2)$ forms the angle $\theta_i$ with respect to the normal $(z)$ to the film plane, and forms the angle $\phi_i$ with respect to the in-plane direction $(x)$ which is perpendicular to the stripes axis $(y)$: see Fig. 3. In our model we assumed $|M_1|=|M_2|=M_S$ where $M_S$ is the Fe saturation magnetization; $\lambda_{12}$ is the exchange coupling between $M_1$ and $M_2$, while $D_{z,i}$ and $D_{x,i}$ are the demagnetizing factors of a given Fe stripe.[13] Since the stripes are very long in the $y$ direction, one has $D_{y,i}\sim 0$ and $D_{z,i}\sim 1-D_{x,i}$. It is useful to describe the action of the shape and magnetic anisotropies on the magnetizations by equivalent dipolar and anisotropy fields, respectively. The dipolar fields $4\pi M_S D_{z,i}$ and $4\pi M_S D_{x,i}$ favor orientation of the magnetization $M_i$ in the film plane $(xy)$ and along the stripes axis $(y)$, respectively. The interface anisotropy $K_{perp}$, arising from the broken translational symmetry along the film normal $(z)$, provides the perpendicular anisotropy field $H_{perp}=\frac{2K_{perp}}{M_S}$ that attempts to orient the magnetization perpendicular to the film plane. The magnetocrystalline anisotropy $K_1$, arising from spin-orbit coupling, has the effect to make energetically favorable for the magnetization to orient along some particular crystallographic directions which differ in various materials and symmetries. In the present case, the

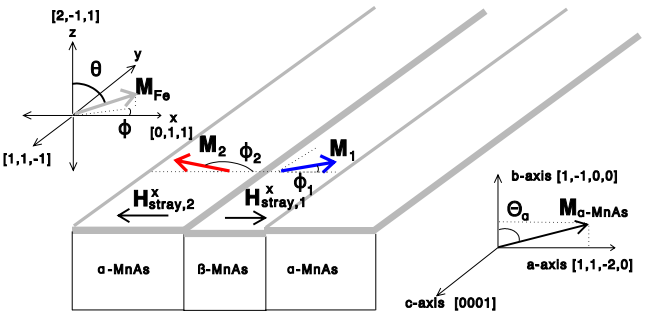


FIG. 3. (Color online) Schematic view of the ultrathin Fe film (light gray) deposited on the striped phase of a thick MnAs/GaAs(001) film with indication of the magnetizations and stray fields. In the insets the reference frame used in the theoretical model is reported.

favored directions lie in the film plane ($xy$) and the equivalent magnetocrystalline anisotropy field is $H_K=\frac{2K_1}{M_S}$. Within the film plane there is also a uniaxial anisotropy $K_{paral}$, induced in the Fe film by the morphology of the MnAs substrate, that favors the $x$ direction and is described by the equivalent uniaxial anisotropy field $H_{paral}=\frac{2K_{paral}}{M_S}$. The external magnetic field $H$ is applied in plane at an angle $\phi_H$ with the $x$ axis. $H_{stray,i}$ $(i=1,2)$ denote the stray fields produced on neighboring Fe stripes by the magnetization $M_\alpha$ of a given $\alpha$-MnAs stripe: $H_{stray,1}$ tends to align $M_1$ parallel to $M_\alpha$ and acts as a bias field on Fe/$\beta$-MnAs while $H_{stray,2}$ tends to align $M_2$ antiparallel to $M_\alpha$ and acts as a demagnetizing field on Fe/$\alpha$-MnAs.

For moderate external fields ($H<2-3$ kOe), $M_\alpha$ is substantially confined to the vertical plane ($xz$), because the stripe axis $y$ is definitely a hard direction (characterized by a strong saturation field of nearly 30 kOe) for MnAs,[14,15] and only the $x$ components of the stray fields are effective. $H_{stray,i}$ are thus determined by the angle $\Theta_\alpha$ that the substrate magnetization $M_\alpha$ forms with $z$. In this respect, our preliminary vibrating sample magnetometry and magneto-optical measurements (not reported here) indicate that, for $T_S$ above 300 K, the remanent MnAs magnetization is not aligned along the $x$ axis, but it is canted, exhibiting an appreciable component normal to the film plane. This behavior is related to the increasing of the shape anisotropy energy with the narrowing of the $\alpha$-MnAs stripes.[13,16] If an external in-plane field is applied, two different behaviors are recognized. When the field $H$ is parallel to $x$, we assume that, starting from the zero-field value $\Theta_\alpha(0)$, the angle that $M_\alpha$ forms with the normal ($z$) to the surface plane increases linearly with $H$,

$$\Theta_\alpha=\begin{cases}\Theta_\alpha(0)+\left[\frac{\pi}{2}-\Theta_\alpha(0)\right]\frac{H}{H_{C,\alpha}}, & H<H_{C,\alpha}\\ \frac{\pi}{2} & H\geq H_{C,\alpha}\end{cases}. \quad (2)$$

Here $H_{C,\alpha}$ is the field value above which $M_\alpha$ lies in the $xy$ plane. Within this scheme, the $x$ components of the stray fields evolve with $H$ according to $H^x_{stray,i}=H^s_{stray,i}\sin\Theta_\alpha$, where the "$s$" apex denotes the saturation value reached for $H\geq H_{C,\alpha}$. In contrast, when $H$ is parallel to $y$, as long as $H$ is smaller than 2–3 kOe, the orientation of $M_\alpha$ remains substantially the same as in $H=0$,[13,14] and the stray fields in Eq. (1) will therefore retain their zero-field values $H^x_{stray,i}(0)=H^s_{stray,i}\sin\Theta_\alpha(0)$.

The equilibrium configuration of $M_1$ and $M_2$ is obtained by setting $\partial F/\partial\eta_j=0$, where $\{\eta_j\}=(\theta_1,\theta_2,\phi_1,\phi_2)$. Owing to the reduced thickness of the Fe stripes, one has $D_{x,i}\ll D_{z,i}$, so that the Fe stripes magnetizations, $M_1$ and $M_2$, always lie within the film plane $xy$ ($\theta_1=\theta_2=\pi/2$). In the top insets of Fig. 2 we show the field dependence of the in-plane angles, $\phi_1$, and $\phi_2$, formed with the $x$ direction by the Fe magnetizations, $M_1$ and $M_2$. One finds that, for a sufficiently high field ($H\gg 2-3$ kOe), $M_1$ and $M_2$ are parallel to $H$ ($\phi_1=\phi_2=0$); as the field intensity is reduced, $M_1$ remains parallel to $H$, while $M_2$ becomes antiparallel ($\phi_2=\pi$) for $H$ smaller than a reversal field $H_{rev}$. Neglecting anisotropies, $H_{rev}$ is given by $|H^s_{stray,2}|$, as discussed later on.[17] In zero external field, $M_1$ and $M_2$ are aligned along $x$, with opposite orientations, under the effect of $H^x_{stray,1}(0)$ and $H^x_{stray,2}(0)$. Then for $H$ applied parallel to $y$, one finds that a complete alignment $\phi_1=\phi_2=\pi/2$ of $M_1$ and $M_2$ can only occur asymptotically because the stray fields $H^x_{stray,i}(0)$ hinder the rotation of $M_1$ and $M_2$.

TABLE I. Values of fitting parameters in the spin-wave energies, Eq. (A2), of the patterned Fe overlayer at two different sample temperatures.

| $T_S$ (K) | $H^S_{stray,1}$ (kOe) | $H^S_{stray,2}$ (kOe) | $H_{C,\alpha}$ (kOe) | $\Theta_\alpha(0)/\pi$ |
|---|---|---|---|---|
| 313 | +0.09 | −1.20 | 0.70 | 0.11 |
| 308 | +0.16 | −0.60 | 0.35 | 0.17 |

The spin-wave frequencies $\omega_1$ and $\omega_2$ can now be calculated assuming small deviations from the equilibrium configuration [see Eqs. (A1) and (A2) in the Appendix]. While the dipolar and anisotropy fields of Fe are known from the analysis of the unpatterned high-temperature phase, the stray fields, $H^s_{stray,i}$, and the direct exchange coupling between stripes, $\lambda_{12}$, are not known for temperatures in which the stripe arrays form, and were treated as fit parameters. Best fit values are reported in Table I. It appears that, with increasing $T_S$, $|H^s_{stray,2}|$ increases while $H^s_{stray,1}$ decreases, consistently with the fact that the $\alpha$-MnAs stripe narrows with increasing temperature. An upper bound of 0.04 kOe was placed on the exchange field $H_{exch}=\lambda_{12}M_S$, corresponding to a negligible dynamic interaction between stripes.

The dependence of the spin-wave frequencies on $H$ applied parallel to $x$ [Figs. 2(a) and 2(c)], can now be understood. The frequency $\omega_1$ monotonically decreases with decreasing $H$ because $M_1$ does not change its parallel orientation in the whole field range. Also the frequency $\omega_2$ decreases with decreasing $H$ as far as $M_2$ is parallel to $x$. At the reversal field $H_{rev}$, $\omega_2$ reaches a minimum and, on further reducing $H$, $\omega_2$ starts to increase, attains a maximum, and finally decreases again. This latter decrease in $\omega_2$ follows [see Eq. (2) and Eq. (A2) in the Appendix] from the $\Theta_\alpha$ dependence of the stray field component $H^x_{stray,2}$. When a sufficiently high field $H$ is applied along $y$ [Figs. 2(b) and 2(d)], both $M_1$ and $M_2$ are forced to align with the field and a single mode is observed. For field values lower than about 1 kOe, $M_1$ and $M_2$ start to rotate away from the field direction and two distinct modes are observed. However, the irregularities in the stripe morphology and the lateral confinement of the in-plane wave vector, which are not taken into account in our analysis, become important at very low-field values and this leads to a worsening of the agreement between theory and experiment.

It is important to note that the step which defines the magnetic stripes has a height less than the Fe thickness so that the Fe stripes are in physical contact with one another. Antiparallel alignment in zero field thus requires the formation of a 180° domain wall separating magnetic domains in adjacent stripes. The formation of domain walls, and their pinning in a parallel array, can be expected as a consequence of the strong stray fields produced by the ferromagnetic

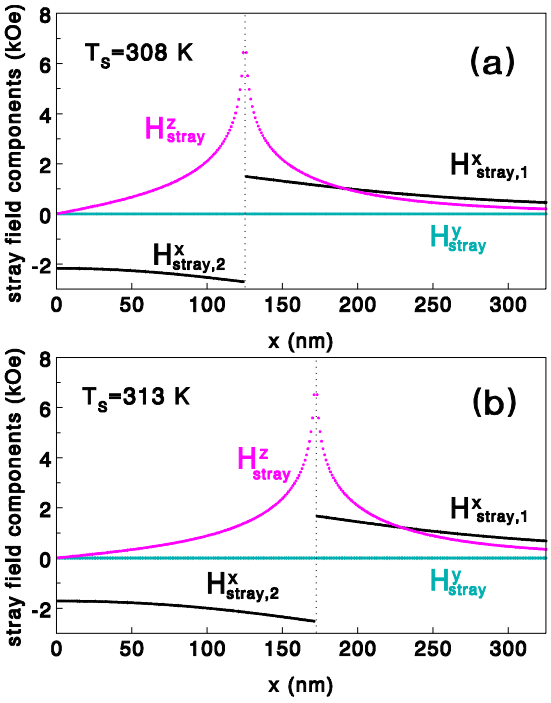


FIG. 4. (Color online) Analytic calculation (Ref. 18) of the $x$, $y$, and $z$ components of the stray field produced by an $\alpha$-MnAs stripe of width $L_{\alpha,x}$ on neighboring Fe/$\alpha$-MnAs ($|x|<L_{\alpha,x}/2$) and Fe/$\beta$-MnAs ($|x|>L_{\alpha,x}/2$) stripes. The length of $\alpha$-MnAs stripe was fixed to $L_{\alpha y}=1000$ nm, the thickness to $L_{\alpha,z}=140$ nm, while the width to $L_{\alpha,x}=325$ nm and 250 nm for (a) $T_S=308$ K and (b) $T_S=313$ K, respectively. The $\alpha$-MnAs magnetization was taken to be constant (670 Oe), directed along $x$. The stray-fields components were evaluated at $y=0$, corresponding to the center of a stripe of finite length $L_{\alpha,y}$, and at $z=70$ nm, corresponding to the upper surface of the $\alpha$-MnAs stripe.

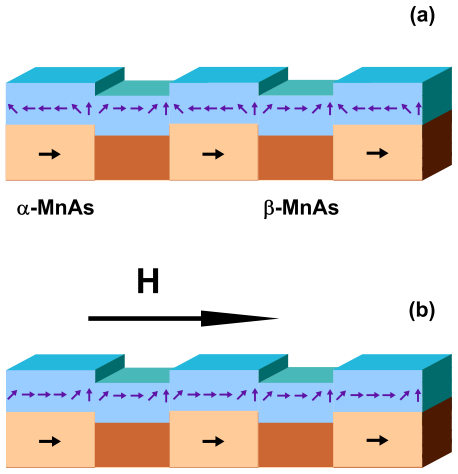


FIG. 5. (Color online) Sketch of the Fe magnetic configuration at (a) low and (b) high applied magnetic field. The $\alpha$-MnAs phase (light orange) is ferromagnetic and large stray fields are produced that affect strongly the Fe film (light blue). The $\beta$-MnAs phase (dark orange) is nonferromagnetic. Note the appearance of 180° domain walls at low applied fields. The walls are suppressed at higher fields when the Fe domains are aligned.

$\alpha$-MnAs stripes. Using an analytic calculation of the magnetic field produced by a bar-shaped $\alpha$-MnAs magnet,[18] we estimated the magnitudes of the stray field components. Results are shown in Figs. 4(a) and 4(b). The very large field normal to the plane of the stripes facilitates the formation of a domain wall in the Fe and, most importantly, pins the wall strongly to the interstripe region. We also note that the calculated values of the $x$ component of the stray fields are in reasonable agreement with the results obtained by our analysis of BLS frequencies.

Micromagnetic calculations using the package OOMMF (Ref. 19) were run to test the pinned wall scenario. At small fields, an antiparallel alignment of neighboring stripe domains was found, separated by a narrow 180° domain wall. The wall structures unwind with increasing applied field and the magnetizations $M_1$ and $M_2$ become parallel above a critical value of the field. A sketch showing the Fe magnetic configuration for an applied field lower and higher than the reversal field is reported in Figs. 5(a) and 5(b), respectively. Neglecting anisotropies for simplicity, the reversal field can be estimated by equating the energies of the antiparallel and parallel configurations, namely: $E_A=-H(M_1L_1-M_2L_2)-H^s_{stray,1}M_1L_1-H^s_{stray,2}M_2L_2+\sigma_A$ and $E_P=-H(M_1L_1+M_2L_2)-H^s_{stray,1}M_1L_1+H^s_{stray,2}M_2L_2+\sigma_P$, where $L_1$ is the width of the Fe/$\beta$-MnAs stripe, $L_2$ is the width of the Fe/$\alpha$-MnAs stripe, and the deformation in the magnetic order near the step region in the two different configurations has associated energy densities $\sigma_A$ and $\sigma_P$. The reversal field is thus estimated to be $H^x_{stray,2}+(\sigma_P-\sigma_A)/(2M_2L_2)$. The second term is small and can be neglected because of the large value of $L_2$ in our experiments, and the smallness of the wall energy difference associated with the magnetic structure near the interface is due to the large normal component of the stray field. In this regard, the 180° domain-wall formation does not affect the reversal field and can be neglected in favor of the larger anisotropy and MnAs stray-field effects. The above considerations provide a mechanism for antiparallel alignment of neighboring Fe stripes in low fields due entirely to the stray fields produced by the MnAs. Therefore this system can be viewed as a lateral exchange spring where Fe/$\beta$ MnAs is the "hard" phase while Fe/$\alpha$ MnAs is the "soft" phase.

As discussed in Ref. 20, domain-wall formation in an exchange-spring structure does not affect strongly spin-wave frequencies for the hard and soft components. The spring serves to stabilize the orientation of the magnetizations in the presence of an applied field and results in a magnetic structure that behaves dynamically like two independent resonators by actually decreasing the penetration length of spin waves from one material into the other. In this regards, our system behaves as a spin-wave isolator and can function as a "spin-wave valve" when an applied field is used to unwind the domain wall and align the magnetizations. For the applied field perpendicular to the stripe axes, at high fields the valve is "closed," in that a large gap exists between the frequencies of spin waves in the two differently oriented domains. At low fields the valve is "open," with a dramatic narrowing of the gap for fields below $H_{C,\alpha}$. This also means that our system can be viewed as an example of artificial magnonic crystal, whose band gap can be "tuned" by either temperature or magnetic field.[2,21,22]

In conclusion, we have shown that a pattern of magnetically independent ferromagnetic stripes can be induced in an ultrathin Fe film using a self-organized MnAs/GaAs(001) template. A quantitative analysis of the spin-wave frequencies provides values for the stray fields due to the $\alpha$-MnAs stripes in addition to other local field contributions. For temperatures where the stripes exist, an antiparallel alignment between Fe domains at low applied fields appears. We argue that a domain-wall structure at the Fe stripe edges isolates statically and dynamically adjacent Fe stripe domains in a manner analogous to a lateral exchange spring.[5] As such, the structure should be of interest for high-frequency properties in the microwave region. Specific applications for microwave device operation may be realized through the field dependence of the resonant absorption. Relatively small magnetic fields can be used in this system to switch between two spin-wave frequency branches, allowing application as a field-sensitive switch or filter, for example. Moreover, the low-field arrangement of parallel domain walls should be of interest for magnetotransport properties and giant magnetoresistance.[23]

## ACKNOWLEDGMENTS

J.M. acknowledges Italian CNR for financial support from Short Term Mobility Program. R.L.S. was supported by the Australian Research Council. Financial support by the Ministero per l'Università e la Ricerca under PRIN-2007 project (Prot. Grant No. 2007X3Y2Y2) is acknowledged.

## APPENDIX

*Calculation of the spin-wave frequencies*. In the uniform mode approximation, the spin-wave resonance frequencies of the Fe overlayer are obtained, for small deviations from equilibrium, as solutions to the biquadratic equations,

$$\det\left\{\frac{\partial^2 F}{\partial\eta_i\,\partial\,\eta_j}+i\omega\left(\frac{M_i}{\gamma}\sin\,\eta_i\delta_{i+2,j}-\frac{M_j}{\gamma}\sin\,\eta_j\delta_{i,j+2}\right)\right\}=0, \tag{A1}$$

where $\gamma$ is the gyromagnetic ratio of Fe, $\delta$ denotes the Kronecker's delta function and in the striped phase one has $\{\eta_j\}=(\theta_1,\theta_2,\phi_1,\phi_2)$. In order to compare with the measured frequencies, one should account for the finite magnon wave vector probed by BLS. For ultrathin films with in-plane magnetization, in the Damon Eshbach (DE) scattering configuration (namely, when the spin wave propagates, with in-plane wave vector $q$, in a direction perpendicular to the in-plane applied magnetic field), this can be accomplished by adding perturbation terms, linear and quadratic in $q$, to the dynamical matrix $\frac{\partial^2 F}{\partial\eta_i\partial\eta_j}$ in Eq. (A1) Such terms are $(-2\pi D_{z,i}M_S qd+\frac{2A}{M_S}q^2)$ for $\frac{\partial^2 F}{\partial\theta_i^2}$, and $[2\pi D_{z,i}M_S qd\,\cos^2(\phi_i-\phi_H)+\frac{2A}{M_S}q^2]$ for $\frac{\partial^2 F}{\partial\varphi_i^2}$, respectively, where $A$ is the exchange stiffness of Fe. This recipe is always valid in the case of a continuous film.[24,25] In the case of a striped Fe film it is valid, *provided that the spin wave propagates along the stripe direction*: this is the DE configuration for the field applied parallel to $x$. For $H$ applied along the stripe axis $y$, the DE spin wave propagating perpendicularly to the field experiences lateral confinement owing to the presence of stripes. While a splitting of the DE mode into a set of discrete lines was observed in arrays of Permalloy wires,[26] such an effect is absent in the case of patterned Fe (Ref. 27) owing to the presence of anisotropy. Thus, in order to analyze the BLS frequency data in the striped phase of Fe/MnAs for $H$ applied along $y$, we tentatively used Eq. (A1): namely, we considered only resonance modes with no corrections in $q^2$ and $q$, corresponding to exchange or dynamic dipolar fields.

*Fitting procedure*. In the fit we assumed $A=2\times10^{-6}$ erg/cm$^3$, $d=4\times10^{-7}$ cm, $q=1.67\times10^5$ cm$^{-1}$, and $M_1=M_2=M_S=1.6$ kOe. Moreover, the intrinsic anisotropy fields of Fe were fixed to the values $H_{perp}=6.5$ kOe, $H_{paral}=0.16$ kOe, $H_K=-0.15$ kOe, obtained by analysis of BLS data relative to high temperatures, outside the range of stripes existence. The demagnetizing factors $D_{x,i}$ $(i=1,2)$ were exactly calculated[12] by modeling Fe stripes as rectangular parallelepipeds of fixed thickness $d=4$ nm, variable width (estimated from the STM measurements) and length 1000 nm (so that $D_{z,i}\sim1-D_{x,i}$). For $T_S=308$ K we estimated $L_2=L_{\alpha,x}=L_1=L_{\beta,x}=325$ nm, then one has $D_{x,1}=D_{x,2}=0.0219$; for $T_S=313$ K, we estimated $L_2=L_{\alpha,x}=250$ nm and $L_1=L_{\beta,x}=400$ nm, then one has $D_{x,1}=0.0183$ and $D_{x,2}=0.0275$. The field dependence of the calculated spin-wave frequencies is plotted in Fig. 2 for $T_S=308$ and 313 K. In the limiting case $\lambda_{12}=0$, which applies to our data, one has simply,

$$\begin{aligned}\left(\frac{\omega_i}{\gamma}\right)^2=&\left\{H\cos(\phi_i-\phi_H)+\left(4\pi M_S D_{z,i}-\frac{2K_{perp}}{M_S}\right)\right.\\&+\left(\frac{2K_{paral}}{M_S}-4\pi M_S D_{x,i}\right)\cos^2\phi_i-\frac{1}{6}\left(\frac{2K_1}{M_S}\right)\\&\times(11\cos^2\phi_i-7\cos^4\phi_i-4)+H^x_{stray,i}\cos\phi_i\\&\left.-2\pi M_S D_{z,i}qd+\left(\frac{2A}{M_S}\right)q^2\right\}\left\{H\cos(\phi_i-\phi_H)\right.\\&+\left(\frac{2K_{paral}}{M_S}-4\pi M_S D_{x,i}\right)(2\cos^2\phi_i-1)-\frac{1}{6}\left(\frac{2K_1}{M_S}\right)\\&\times(29\cos^2\phi_i-28\cos^4\phi_i-4)+H^x_{stray,i}\cos\phi_i\\&\left.+2\pi M_S D_{z,i}qd\cos^2(\phi_i-\phi_H)+\left(\frac{2A}{M_S}\right)q^2\right\}\\&-\frac{1}{2}\left(\frac{2K_1}{M_S}\right)^2(9\cos^6\phi_i-12\cos^4\phi_i+4\cos^2\phi_i).\end{aligned} \tag{A2}$$

*tacchi@fisica.unipg.it

[1] E. F. Kneller and R. Hawig, IEEE Trans. Magn. **27**, 3588 (1991).
[2] S. Neusser and D. Grundler, Adv. Mater. **21**, 2927 (2009).
[3] E. E. Fullerton, J. S. Jiang, and J. S. Bader, J. Magn. Magn. Mater. **200**, 392 (1999).
[4] M. Grimsditch, R. Camley, E. E. Fullerton, S. Jiang, S. D. Bader, and C. Sowers, J. Appl. Phys. **85**, 5901 (1999).
[5] J. McCord, L. Schultz, and J. Fassbender, Adv. Mater. (Weinheim, Ger.) **20**, 2090 (2008).
[6] L. Däweritz, Rep. Prog. Phys. **69**, 2581 (2006); R. Engel-Herbert, T. Hesjedal, J. Mohanty, D. M. Schaadt, and K. H. Ploog, Phys. Rev. B **73**, 104441 (2006), and references therein.
[7] R. Breitwieser, F. Vidal, I. L. Graff, M. Marangolo, M. Eddrief, J.-C. Boulliard, and V. H. Etgens, Phys. Rev. B **80**, 045403 (2009).
[8] R. Breitwieser, M. Marangolo, J. Lüning, N. Jaouen, L. Joly, M. Eddrief, V. H. Etgens, and M. Sacchi, Appl. Phys. Lett. **93**, 122508 (2008).
[9] M. Sacchi, M. Marangolo, C. Spezzani, L. Coelho, R. Breitwieser, J. Milano, and V. H. Etgens, Phys. Rev. B **77**, 165317 (2008).
[10] http://ghost.fisica.unipg.it/
[11] M. Grimsditch, S. Kumar, and E. E. Fullerton, Phys. Rev. B **54**, 3385 (1996).
[12] The latter feature is confirmed by recent ferromagnetic resonance data [J. Milano (unpublished)].
[13] A. Aharoni, J. Appl. Phys. **83**, 3432 (1998).
[14] J. Lindner, T. Tolinski, K. Lenz, E. Kosubek, H. Wende, K. Baberschke, A. Ney, T. Hesjedal, C. Pampuch, R. Koch, L. Däweritz, and K. H. Ploog, J. Magn. Magn. Mater. **277**, 159 (2004).
[15] L. B. Steren, J. Milano, V. Garcia, M. Marangolo, M. Eddrief, and V. H. Etgens, Phys. Rev. B **74**, 144402 (2006).
[16] L. N. Coelho, B. R. A. Neves, R. Magalhaes-Paniago, F. C. Vicentin, H. Westfahl, R. M. Fernandes, F. Iikawa, L. Däweritz, C. Spezzani, and M. Sacchi, J. Appl. Phys. **100**, 083906 (2006).
[17] In the presence of anisotropies, one has that $\phi_2=0$ is a minimum for $H > |H^s_{stray,2}|+4\pi M_s D_{x,2}-H_{paral}-\frac{1}{2}\ H_K$ and $\phi_2=\pi$ is a minimum for $H\langle H^s_{stray,2}|-4\pi M_s D_{x,2}+H_{paral}+\frac{1}{2}\ H_K$.
[18] R. Engel-Herbert and T. Hesjedal, J. Appl. Phys. **97**, 074504 (2005).
[19] http://math.nist.gov/oommf/
[20] K. L. Livesey, D. C. Crew, and R. L. Stamps, Phys. Rev. B **73**, 184432 (2006).
[21] M. Krawczyk and H. Puszkarski, Phys. Rev. B **77**, 054437 (2008), and references therein.
[22] Z. K. Wang, V. L. Zhang, H. S. Lim, S. C. Ng, M. H. Kuok, S. Jain, and A. O. Adeyeye, Appl. Phys. Lett. **94**, 083112 (2009).
[23] J. F. Gregg, W. Allen, K. Ounadjela, M. Viret, M. Hehn, S. M. Thompson, and J. M. D. Coey, Phys. Rev. Lett. **77**, 1580 (1996).
[24] J. F. Cochran, J. Rudd, W. B. Muir, B. Heinrich, and Z. Celinski, Phys. Rev. B **42**, 508 (1990).
[25] G. Carlotti and G. Gubbiotti, Riv. Nuovo Cimento **22**, 1-60 (1999).
[26] J. Jorzick, S. O. Demokritov, B. Hillebrands, M. Bailleul, C. Fermon, K. Y. Guslienko, A. N. Slavin, D. V. Berkov, and N. L. Gorn, Phys. Rev. Lett. **88**, 047204 (2002).
[27] S. M. Chérif, Y. Roussigné, C. Dugautier, and P. Moch, J. Magn. Magn. Mater. **222**, 337 (2000).